EFDA–JET–CP(13)01/06

A. Widdowson, E. Alves, C.F. Ayres, A. Baron-Wiechec, S. Brezinsek,
N. Catarino, J.P. Coad, K. Heinola, J. Likonen, G.F. Matthews, M. Mayer,
M. Rubel and JET EFDA contributors

Material Migration Patterns and Overview of First Surface Analysis of the JET ITER-Like Wall

Material Migration Patterns and Overview of First Surface Analysis of the JET ITER-Like Wall

A. Widdowson[1], E. Alves[2], C.F. Ayres[1], A. Baron-Wiechec[1], S. Brezinsek[3], N. Catarino[2], J.P. Coad[4], K. Heinola[5], J. Likonen[4], G.F. Matthews[1], M. Mayer[6], M. Rubel[7] and JET EFDA contributors*

JET-EFDA, Culham Science Centre, OX14 3DB, Abingdon, UK

[1]EURATOM-CCFE Fusion Association, Culham Science Centre, OX14 3DB, Abingdon, OXON, UK
[2]Associação EURATOM/IST, Instituto de Plasmas e Fusão Nuclear, Instituto Superior Técnico, Universidade de Lisboa, Avenue Rovisco Pais, 1049-001, Lisboa, Portugal
[3]Association EURATOM-Forschungszentrum Jülich, IPP, D-52425, Jülich, Germany
[4]Association EURATOM-TEKES, VTT, PO Box 1000, 02044 VTT, Espoo, Finland
[5]Association EURATOM-TEKES, University of Helsinki, PO Box 64, 00014 University of Helsinki, Finland
[6]Max-Planck-Institut für Plasmaphysik, EURATOM Association, 85748 Garching, Germany
[7]Royal Institute of Technology, Association EURATOM-VR, 100 44 Stockholm, Sweden
** See annex of F. Romanelli et al, "Overview of JET Results", (24th IAEA Fusion Energy Conference, San Diego, USA (2012)).*

Preprint of Paper to be submitted for publication in Proceedings of the 14th International Conference on Plasma-Facing Materials and Components for Fusion Applications, Jülich, Germany.
13th May 2013 - 17th May 2013

ABSTRACT

Following the first JET ILW operations a detailed in situ photographic survey of the main chamber and divertor was completed. In addition, a selection of tiles and passive diagnostics have been removed from the vessel and made available for post mortem analysis. From the photographic survey and results from initial analysis, the first conclusions regarding erosion, deposition, fuel retention and material transport during divertor and limiter phases are drawn. The amount of deposition on inner and outer base divertor tiles and remote divertor corners has reduced by more than an order of magnitude. Deuterium retention ratio in mainly beryllium deposits has reduced by a factor of five and carbon concentrations are low. There is however beryllium deposition at the top of the inner divertor. The net beryllium erosion rate from the midplane inner limiters is found to be higher than for the previous carbon wall campaign although further analysis is required to determine the overall material balance due to erosion and re-deposition.

1. INTRODUCTION

The ITER-like Wall (ILW) campaign ran from September 2011 - July 2012 [1]. It was the first campaign following the complete change of the interior wall of the vessel from a carbon (C) wall to an all metal wall. In the main chamber the all metal wall consists of solid beryllium (Be) inner and outer limiters and upper dump plate tiles, as well as some recessed limiter tiles with tungsten (W) surfaces. In addition, Be coated inconel tiles are installed at a selection of recessed limiters and as inner wall cladding between the inner limiters. In the divertor the tiles were made from carbon fibre composite (CFC) coated with a 20μm W coating [2].

Prior to installing the ILW tiles, a subset of them were assigned for future post mortem analysis. These tiles received special marker coatings. For Be tiles in the main chamber this was a 2μm Ni/8μm Be marker layer and for the W-CFC divertor tiles this was either (i) a modified W coating structure with a thinner surface W layer (3μm Mo/12μm W/4μm Mo/4μm W), or (ii) an outer Molybdenum (Mo) coating (3μm Mo/12μm W / 4 μm Mo) to allow for post mortem analysis of W migrating onto the Mo surface. These marker coated tiles were pre-characterised prior to installation in the vessel in order that post mortem analysis on removal would elucidate the surface changes due to material migration, erosion, deposition and fuel retention. Results from the post mortem analysis gives integral data over a campaign which in turn provides vital data for comparison with observations from in-vessel experiments. For example for gas balance measurements [3] - which provides the long-term retention related to one day and one single plasma configuration - post mortem analysis can be used to quantify long term fuel retention. Post mortem analysis can also be used to quantify oxygen(O) and C present in deposits and therefore assist in evaluating the findings of the initial in-vessel conditioning cycle with baking and deuterium (D) glow discharge [4] and the regularly repeated monitoring discharges [5]. In these experiments a reduction in O and C levels was indicated during plasma operation in the JET-ILW by more than one order of magnitude compared with the JET-C wall.

2. EXPERIMENTAL DETAILS

The intervention following the first ILW campaign ran from August 2012 - April 2013. In this time full remote handling (RH) access was available in the vessel. One of the first activities during the intervention was to utilise RH to complete a stereo-photographic survey of the inside of the vessel. The stereo images are used to check the configuration model of JET and also provide a comprehensive survey of the condition of the inside of the machine. From these photographs various features on tiles have been identified which are indicative of the initial material migration and erosion/deposition patterns evolving in the machine.

In addition to the full in situ stereo-photographic survey a set of tiles were removed from the JET vessel. The removed tiles were generally those assigned as markers as discussed in Section 1 and were representative of a poloidal cross section around the main chamber wall and the divertor. The tiles in the main chamber were a selection from the inner wall guard limiters (IWGL), wide poloidal limiters (WPL) at the outer wall, upper dump plates (DP) at the top of the vessel and inner wall cladding (IWC) recessed behind the IWGLs, see Figure 1. The tiles from the divertor were namely tiles 1, 3, 4, 5, 6, 7, 8 and in addition a high field gap closure tile (HFGC) inboard of the top of the inner divertor and a tile B and tile C outboard of the outer divertor as indicated in red in Figure 1 and shown in detail in Figure 2. Toroidal symmetry is not studied here. Due to time constraints first results for the IWC tiles and Tile 5 are not available at the time of writing and are therefore not discussed here.

As well as the removal of tiles, a series of passive erosion/deposition diagnostics were removed and replaced in the vessel. The diagnostics include rotating collectors, sticking deposition monitors, louvre clips and mirrors. The locations of these diagnostics are indicated in Figure 1 and Figure 2.

The results presented here and elsewhere [6] [7] [8] provide the initial findings of a subset of the tiles and diagnostics available. The analysis techniques used include Ion Beam Analysis (IBA), in particular Nuclear Reaction Analysis (NRA) and Proton Back Scattering and Proton Induced X-ray Emission primarily at IST in Portugal and IPP Garching in Germany, surface profiling at CCFE in the UK and Secondary Ion Mass Spectroscopy at VTT in Finland. Details of these techniques can be found elsewhere [6][9].

In order to compare the results following the JET-ILW campaign with the JET carbon wall (JET-C) data it is necessary to understand differences between the two operating periods. The plasma statistics for the divertor phase and the limiter phase for the different operating periods are summarised in Table 1; 2005-2007 and 2008-2009 are for the JET-C campaigns and 2011-2012 for the JET-ILW campaign. It should be noted that this is the total time for all operations, including commissioning pulses and does not take into account variations in input power or other plasma parameters such as particle fluxes responsible for initial sputtering. The proportion of limiter phase for the ILW is slightly higher than for the JET-C. This is due to a number of dedicated limiter plasma experiments performed in JET-ILW to test the operating limits of the Be first wall in the main chamber [10], (ii) gas balances in limiter configuration [11] and (iii) sputtering experiments [12]. No such experiments

took place in JET-C in the period mentioned for comparison. In addition, for pulses starting with limiter phases and moving to divertor phase the overall limiter and divertor phase times were decreased during the JET-ILW operations when compared with JET-C.

3. RESULTS

In this section details from the in-vessel and additional close up photographic surveys and key results from the post mortem analysis of tiles and diagnostics are presented. They are divided into separate tile types for clarity to give a Tour of the Torus.

3.1. INNER WALL GUARD LIMITERS

Following a dedicated experiment of limiter phase plasmas to test the operational limits of the Be first wall strong melting was observed at the upper mid-plane region on four of the inner limiter beams. The melting occurred at the lower edge of the tile located at the central ridge running toroidally along the tile and was consistent with the heat flux distribution showing the contact point of the plasma on the limiter [10]. The melting was strong enough that molten material travelled a considerable distance across at least two tiles in an upward poloidal direction due to $j \times B$ Lorentz forces and plasma pressure as discussed in [13].

Arc tracks were observed on the ends of the IWGL tiles. For tiles at the mid-plane and lower, arcing was visible on both the left and right ends of the IWGL tiles. Above the mid-plane arc marks were observed on the left end of the tiles only. Photographs of the arc tracks on the ends of the IWGLs are shown in Figure 3(a) & (h). In general, arc tracks are oriented at 10° to 15° (clockwise) on the left end of the tiles with respect to the IWGL beam vertical axis, and −20° to −30° (anti-clockwise) on the right end of the tile as indicated by the blue arrows in Figure 3. This pattern of arc tracks on left and right ends of the IWGL tiles was similar in all of the IWGL tiles where arcing was observed. The path of the arc tracks is dependent on the magnetic field direction and the curved surface of the tiles and can be classified as linear arcs as shown in [14].

Dark deposition patterns were observed on the left and right ends of the IWGL tiles but not on the central part of the tile. Tiles below the mid-plane have a dark deposition on both ends of the tiles, whereas the upper tiles have a dark deposition only on the right end of the tiles, as shown in Figure 3(h) and indicated by grey shading. During the intervention these deposits were sampled using an abrasive pad. It was found that the deposits were easily removed and are therefore loosely adhered to the tile surface. Surface profiling indicates that they are very thin [8].

Other changes to the surface morphology were also observed as shown in Figure 3. These include various degrees of Be melting resulting in material bridging gaps between castellations on the tile surfaces and melt flow upwards on the central ridge (Figure 3(c)), melting of castellation edges (Figure 3(d)), a convoluted fern-like feature probably due to arcing (Figure 3(b)) [14] and general surface roughening (Figure 3(e) & (f)). In general the morphological changes observed follow the diagonal heat flux distribution running from top right through the central region to the bottom left

as discussed in [10]. In addition the changes appeared more extensive on the tiles in the region just above the mid-plane on the inner limiter.

An additional feature was a pronounced plane wave structure vertically aligned observed in the regions left and right of the centre of the tile (Figure 3(f) & (g)). These are probably related to the surface finish due to electro discharge machining which was used in the manufacturing process for the tiles. The vertical lines from the surface finish have been accentuated during exposure to the plasma. It is not yet understood why the surface modulations which are on the scale of microns have become more visible following the JET-ILW campaign.

As with the surface morphology effects of heating, melting and arcing, the erosion and deposition pattern on the IWGL follows the diagonal heat flux distribution [10] and in that respect is similar to the IWGL deposition and erosion pattern in JET-C [15]. Surface profiler measurements indicate deposit on the right end and erosion from the centre of a mid-plane IWGL tile [8]. IBA results on either end of the tile of the same inner limiter tile from the mid-plane also indicate the presence of either a band of deposit or a band of melted and re-solidified Ni/Be marker coating on the right side of the tile and a thinner deposit which looks to have melted on the left side of the tile. At the very ends of the IWGL tile there is no plasma interaction apart from the arcing discussed earlier. This is to be expected as the tile ends are further into the scrape-off layer (SOL).

Taking the results from surface profiling and IBA, a first estimate of net erosion rate can be made from the inner limiter mid-plane tiles. Assuming one row of tiles on ten limiters from the Be inner limiter compared with sixteen C inner limiters and normalising to the plasma operational time in limiter configuration the erosion rate for Be is 2.3×10^{19} atoms s^{-1} which is slightly higher than for JET-C, 1.4×10^{19} atoms s^{-1}. This erosion rate is a first approximation for comparing erosion from the Be limiters of the JET-ILW with the carbon limiters in JET-C. Other parameters such as self sputtering with Be at low density operation, incident flux, temperature, power and variations in the point of contact of the plasma with the inner limiters also influence erosion rates. It must also be noted that this is the result for one row of mid-plane tiles and is not therefore indicative of a net erosion source - the overall erosion and deposition balance for the main chamber is still to be determined.

3.2. UPPER DUMP PLATES

Extensive melting occurred along the poloidal ridge of the upper dump plate (DP) tiles. Unlike the melting on the IWGL which only occurred on four of the inner limiters indicating asymmetry in the plasma surface interaction with the limiters, the melting of the DP was found at all locations around the top of the machine and was therefore toroidally uniform. Melting such as this provides an additional Be erosion source and indeed droplets were observed on divertor tiles. The droplets were millimeters in size. However the density of droplets in the divertor was not high; during the refurbishment of 1/12th of the divertor tiles the close up photographic survey revealed tens of 10 droplets. The number is probably low as droplets falling from the DP during a pulse act as a Be

impurity source for the plasma. Molten Be droplets will only reach the divertor once the plasma has subsided. Due to the extensive melting of the DP tiles it may not be possible to quantify the erosion/deposition of the tile from surface profiling measurements [8].

3.3. WIDE POLOIDAL LIMITERS

The in-vessel photographic survey shows additional areas of strong melting located near the top of the limiter beam on four limiters [10]. For the WPL tiles the molten material moves downwards at an angle due to the j×B Lorentz forces plasma pressure [13].

Visual inspection of the WPL tiles removed from the vessel has shown similar arc markings on the left and right ends of an upper WPL tile, however the arc tracks have a different orientation to that seen on the IWGL tiles; they are oriented upwards and outwards from the vertical axis of the WPL beam as seen in Figure 4. The difference between the arc tracks at the inner and outer walls is related to the magnetic field direction and the curvature of the tile as shown in [14]. On a mid-plane WPL tile there is evidence of erosion from the central region of the tile and a deposition band towards the ends of the tile. Detailed analysis of the three WPL tiles removed from the vessel is still to be completed.

To the sides of the WPLs there are protection tiles fabricated from W-coated CFC. Arcing has been observed on the top protection tiles in two locations. Along the arc tracks also dark patches of the order of 1mm in diameter are observed where the coating has been breached by the arc to the CFC substrate [16]. It is expected that the patches will reveal higher concentration of C when detailed analysis is completed.

One of the few areas showing failure of the order of 20% of the W-coated surface is at the neutral beam reionisation protection tiles located at the sides of two outer limiters in the mid-plane. These tiles intercept fast ions generated by ionisation of neutral beam particles near the plasma edge. The coating on these tiles is peeling away from the surface and appears to follow the CFC fibre structure as shown in Figure 5. A decreasing concentration of Be radially out from the centre of the machine has been measured using IBA on this tile. At this stage it is not known whether the presence of Be deposit on the W-coating contributes towards the failure of the coating by way of the formation of alloys or whether the failure is related to other interactions or an adhesion problem. Further details of W-coated CFC tiles from around the vessel are discussed in [16].

3.4. DIVERTOR

The results for the deposition of the inner divertor tiles 1, 3, 4 and the outer divertor base tile 6 are presented here. The location of these tiles in the JET divertor is shown in Figure 2.

3.5. INNER AND OUTER BASE DIVERTOR TILES

On both horizontal tile 4 at the inner and tile 6 at the outer divertor silvery deposits were observed on the sloping part of the tile which is accessible to the plasma. These films look thin and this is

confirmed from the IBA analysis showing the amount of Be on the sloping surface of tile 4 as ~3×10^{18} atoms cm^{-2} (250nm - assuming ρ_{Be} = 1.85g/cm^3) and along a toroidal band at the bottom of the sloping surface ~6×10^{17} atoms cm^{-2}. The thickness of the deposits are two orders of magnitude less than for a tile in the same location in JET-C. In JET-C deposits > 100 μm occur on the sloping part of the tile and also on the remote horizontal surface of the tile.

3.6. INNER DIVERTOR VERTICAL TARGET TILES

In contrast to tiles 4 and 6 there is a significant amount of deposit on the top horizontal surface (apron) of tile 1 and the top third of the plasma facing surface of tile 1 at the inner divertor. From IBA the deposit is shown to be predominantly Be [6]. As the deposits exceed the interaction volume of the NRA technique surface profiling is used to evaluate the thickness of the deposit on the top plasma facing surface. The deposit is found to be 10 – 15μm ± 5μm [8]. It was not possible to profile the apron of tile 1 using the profiling technique due to difficulties in orientating the surface for analysis, therefore it is assumed that the thickness of the deposit in this region is similar to that on the top front surface by comparing the Be concentration from NRA, i.e. of the order 10 μm. For the remaining part of tile 1 the NRA data indicates negligible deposit whereas surface profiles indicate that deposits as thick as 10 μm ± 5 μm are possible. This data requires further evaluation. Further microscopy data will be used to make the final evaluation of the erosion/deposition for tile 1.

The vertical plasma surface of tile 3 (below tile 1) has been evaluated by surface profiling [8] and IBA [6]. IBA indicated a very thin deposit < 1 μm and surface profiling indicates 5 μm ± 5 μm. The deposits on the apron are thin when compared with the deposits seen for JET-C on the same surface (98 μm for 2005-2007 and 50μm for 2008-2009). However when this is scaled with the divertor plasma time the Be deposition
rate on the top of tile 1 is 3.3×10^{15} atoms cm^{-2} s^{-1} for the JET-ILW compared with 3.9×10^{15} atoms cm^{-2} s^{-1} (2005-2007) and 1.5×10^{15} atoms cm^{-2} s^{-1} (2008-2009) for C deposition in a similar location in JET-C. Thus the Be deposition rate appears higher for the JET-ILW than the C deposition rate for the most recent 2008-2009 JET-C campaign and similar to the deposition rate in the 2005-2007 JET-C campaign.

3.7. TUNGSTEN COATINGS ON DIVERTOR TILES

Following the ILW campaign the W coatings in the divertor have been extensively photographed and from photography look largely intact. However there are two areas where delaminations have been observed; on the apron of the outer divertor tile 8 and the inner edge of the top horizontal surface of tile 6. These locations are indicated in Figure 2. The delaminations follow the lamination grain of the CFC. The in-vessel photographic survey shows that there is no systematic pattern emerging for these delaminated areas. This indicates that the areas of delaminations are probably related to the variable CFC surface resulting from material manufacture or machining. Further investigation [16] and monitoring of the W coatings is continuing. The total area of delaminations is extremely

small and not significant as a source of carbon but the W particles generated may contribute to transient impurity events [17].

Another phenomenon is arcing on the top horizontal surface of tile 4. Here thin films with a blue colour are observed around the vessel. In the blue coloured deposits arc tracks are clearly seen running radially from the machine central axis. The presence of arc tracks in this location could be due to an insulating deposit containing nitrogen (N) from inner divertor N_2 puffing experiments [18]. There is evidence of higher levels of N on mirror samples at the inner divertor corner [7]. Further analysis of this tile is required to confirm whether elevated amounts of N are found on tile 4.

3.8. DUST AT THE INNER AND OUTER DIVERTOR SURFACES

One of the first actions to be completed in the intervention following the ILW campaign was the collection of dust from the divertor tile surfaces. The dust collection was split into two vacuuming samples as the quantity of dust was expected to be small; one from the inner divertor (including tiles HFGC, 1, 3, 4) and one from the outer divertor (tiles 5, 6, 7, 8). The surfaces are indicated in red and blue respectively in Figure 2. Access to the remote louver regions was not possible during this intervention. The amount of dust collected from the inner and outer divertors are 0.7 g and 0.3 g respectively compared with 137 g and 51 g from the inner and outer divertor from a similar surface area from JET-C after 2008-2009 operations.

As many divertor tiles in JET-C were in the vessel since 1998 the dominant mechanism for producing dust and flakes in the divertor for JET-C was from spalling deposits that have reached a critical thickness. In contrast the deposition rate for material migrating to the divertor in the JET-ILW is at least an order of magnitude less than for JET-C. Consequently the deposits forming in the divertor are thin and have not reached a stability limit where spalling occurs resulting in only a small amount of dust being collected. The dust that was collected is therefore likely to come from other sources such as W-coating delamination and Be melting in the main chamber. It is important to continue to monitor dust quantities and layer growth in the divertor in future JET interventions through dust collection and post mortem analysis to build up an accurate picture of dust production, material migration and material balance. The reduction in material migration to the divertor indicates that it will take longer in the JET-ILW to come to a steady state condition for the production of dust from spalling deposits.

3.9. REMOTE DIVERTOR CORNERS

The remote divertor corners consist of the ribs supporting the divertor tiles (indicated by dark blue circles in Figure 2) and the cooled louvers (indicated by dark blue triangles in Figure 2) which form part of the divertor structure and lie behind the ribs. These regions are remote to the plasma and several diagnostics are located in these areas to monitor deposition. The close up photographic survey reveals thin films that have formed at the remote areas of both the inner and outer divertor. At the inner divertor the films are thin and coloured interference fringes are observed on the passive

diagnostics and the C ribs. At the outer divertor the coating is silvery and coats the diagnostics and the ribs. Some evidence of flaking is observed on a cover and on a
mirror located at the outer ribs, which could indicate thicker coatings in limited locations.

NRA was used to evaluate deposits on two stainless steel covers which protected two sticking monitors, one at the inner and one at the outer divertor ribs. The results for the covers from the ILW show that the deposits in this area are reduced by at least an order of magnitude compared to JET-C samples. For example, for the covers removed at the end of JET-C campaign the deposit on the covers were spalling, indicating that films were at least 10 μm thick and new layers were growing on exposed surfaces after spalling. For the ILW the layers on these covers are of the order of 200nm thick. Deposits of the order of 500nm were observed on mirrors in the same regions [7]. In JET-C significant C deposition was found in these regions as C was able to migrate via chemical erosion with the deuterium fuel to these areas.

Be, C, D and W are present in the films - the quantification of the C and W is still on going. It should be noted that the source of C could be due to the proximity of the C ribs (these were not coated prior to the ILW campaigns) and also the initial C in the machine that has been shown to decrease during the first few weeks of the ILW campaign. Despite these sources the amount of C in the remote areas in low. It is expected that W will be present in significant amounts at the outer divertor due to line of sight erosion when the outer strike point [5]. The total amount of deuterium does not vary significantly between the inner and outer corners. For the JET-ILW the maximum value of D/Be = 0.2, for JET-C D/C = 1. Further analysis to determine the C concentration is required before the D/C ratio for the ILW can be quoted. Additional results from the remote louvers region are discussed in [7].

4. DISCUSSION

4.1. MATERIAL MIGRATION DURING LIMITER PLASMA

During the limiter phase of the plasma material will be eroded from the limiters and deposited within the main chamber creating a likely overall balance. The results presented here show that the erosion rate from the inner limiter tiles located at the mid-plane is higher than for JET-C during the limiter phase. Considering just one row of tiles from the mid-plane and 10 limiter beams the net erosion is 7g of Be, this compares with 11g for JET-C from one row of tiles on 16 limiter beams, summarised in Figure 6. Taking into account the total duration of limiter plasmas for the two campaigns the difference in the net erosion rate at the mid-plane between the JET-ILW and JET-C is less marked although still higher for the Be wall as discussed in Section 3.1.

Whilst strong erosion sources from the mid-plane inner limiters have been identified further analysis is required to identify regions of deposition in the main chamber. For JET-C the extremities of the inner limiter (i.e. the top and bottom of the limiter) were shown to be a region of net deposition [9] as shown in Figure 6 where 0.8g of C was deposited on one row of tiles at the top of the limiter. This is of the order of 1% of the erosion from the mid-plane limiter row. For the ILW,

surface profiling results on an upper IWGL tile indicate very little interaction with the plasma [8]. The results are < 5μm of either erosion or deposition and less than the resolution of the equipment, so no clear conclusion can de drawn whether deposition occurs from these results, but clearly the ends of the limiter are not a significant deposition area.

An additional region of Be deposition has been identified on the neutral beam re-ionisation protection tiles on the outer limiter beams which require further quantification.

In order to make a complete evaluation of the material erosion and deposition balance in the main chamber further analysis of tiles from the inner and outer limiters, upper dump plates and the inner wall cladding is required as indicated in Figure 6.

4.2. MATERIAL MIGRATION DURING DIVERTOR PLASMA

For JET-C it is known that energetic charge-exchange neutrals, fluxes of ions during edge localised modes (ELMs) and chemical erosion contributed to the C source from the main chamber during the divertor phase [19]. Erosion due to charge-exchange neutrals and ELMs is expected to continue for the ILW however the source from the Be wall is expected to be lower as an energetic threshold exists for the sputtering of Be [12]. However the chemical sputtering mechanism by which C erodes is no longer present for Be. Results from the divertor tiles are broadly in line with this hypothesis. For example, comparing the inner and outer divertor tiles 4 and 6, the volume of deposit (see Table 2) on these tiles is two orders of magnitude lower in JET-ILW than JET-C. There is also at least an order of magnitude reduction in deposit reaching the remote divertor areas since the stepwise transport of hydrocarbons is no longer applicable. In contrast at the top of tile 1 at the inner divertor there is a significant deposit and the rate of deposition on the apron of tile 1 during the divertor plasma appears higher for the ILW than for the last C wall campaign (2008-2009) and similar to the deposition rate during the 2005-2007 C wall campaign, as shown in Section 3.6. Initially this may seem contrary to the expected reduction in Be erosion from the main chamber but in fact this might be expected as a high fraction of the C deposited on tile 1 was either (i) re-eroded and migrated to tile 4 and the remote inner divertor corner resulting in thick spalling deposits or (ii) was directly spalling from the apron region. Consequently the true C deposition rate on tile 1 is likely to be higher than calculated. These initial results are encouraging and even with significant deposition on tile 1 an overall reduction in deposition in the divertor for the ILW is observed.

From the divertor deposition results a calculation can be made to estimate the upper limit of the Be erosion rate assuming that the amount of Be eroded from the main chamber during the divertor phase must balance with the amount of deposit in the divertor. Using the values from Table 2 the deposit in the divertor is ~25.8 cm^3. An equivalent volume of Be eroded from the inner wall surface of the main chamber - approximately 21 m^2 in area - would be achieved with an erosion depth of the order of 1.2μm giving an erosion rate of 25.6×10^{-6} μm/s for the divertor phase. This upper limit for the erosion rate is lower than for JET-C where erosion from the main chamber IWC tiles for 2005–2009 was 8μm [19], equivalent to an erosion rate of 37.0×10^{-6}μm/s and scaling for 2008

–2009 to give a total C erosion mass of 129g (Figure 6). There are a number of uncertainties to be considered in this calculation. Firstly the amount of material on the apron of tile 1 not precisely known from the IBA or surface profiling - further cross section microscopy is required to make the final evaluation. Secondly the calculated erosion value assumes that the erosion source due to the divertor phase is from the IWC and does not consider the DP or WPL surfaces as possible wall sources. For JET-C DP tiles were considered as a significant source of erosion (130g for all DP tiles shown in Figure 6) based on the complete removal of a 10μm C marker coating [9]. However the source from the WPL was only 3.1g (see Figure 6). Including these surfaces would decrease the erosion rate from the main chamber tiles. Therefore the assumption that the IWC is the sole main chamber source gives an upper value for the erosion rate. To fully evaluate the Be source during the divertor phase characterisation of the inner wall cladding is required along with spectroscopic data from the main chamber plasma during the divertor and limiter phases.

The distribution of the strike point during the ILW campaign compared to previous campaigns is expected to influence the distribution of deposited material around the divertor. For the ILW campaigns the inner strike point was consistently held on the top of tile 3 putting the apron and top plasma facing surface of tile 1 into the SOL. This may explain why deposit is not observed on the inner base divertor tile 4, as the strike point was not on this tile for any extensive period of time during operations. In addition the lack of step-wise transport due to chemical erosion of deposited material on the inner divertor also reduces the amount of material reaching tile 4 and remote areas.

CONCLUSIONS

Following the JET ILW campaign and the subsequent intervention a set of tiles and passive diagnostics have been removed from the machine for analysis. The analysis programme began in February 2013 and has given a snap shot of the initial Be erosion and deposition results. Based on these initial results it has been possible to draw the first conclusions on material migration, erosion/deposition trends and fuel retention for the JET-ILW and make comparisons with JET-C.

The mid-plane inner limiter is found to be a net erosion zone as a result of interaction with limiter plasmas. The erosion rate of Be from this region is higher than for JET-C. However significant regions of deposition in the main chamber for the material eroded during the limiter phase have yet to be established. There is evidence of a small amount of deposition at the ends of the inner limiter tiles and also at the sides of the outer limiters but this is not fully quantified. Therefore a material balance between erosion and deposition during limiters plasmas has not yet been established.

Overall deposition in the divertor during the divertor plasma is reduced. Although a significant amount of deposit is observed at the top of the inner divertor the deposition in the base divertor is at least two orders of the magnitude lower than for JET-C and the migration of material to remote areas is at least an order of magnitude lower. These results indicate that material deposited at the divertor during divertor plasmas is not migrating via step-wise re-erosion and re-deposition from the inner vertical targets to the base divertor or into remote areas. The absence of Be sputtering at

low impact energies is likely to inhibit the transport to remote areas which is contrast to chemical sputtering of C by hydrogen isotopes. There is also a reduction of at least a factor of five in the D/Be ratio in deposits in remote areas of the ILW compared with the D/C ratio in similar remote areas in JET-C.

A photographic survey of the JET vessel has revealed areas of melting on main chamber Be tiles, most of it shallow, and some areas of delamination of W coatings on W-coated CFC tiles in the divertor. There is also evidence of arcing at various locations around the vessel, notably the wing tiles on the inner and outer poloidal limiter tiles and tile 4 divertor tiles. All these features act as additional erosion sources if the main chamber and divertor. However it should be noted that the W coating in the divertor show no significant delamination and none that appears due to plasma operations and that the Be melting in the main chamber is largely thought to originate from a particular experiment investigating the operating limits of the wall.

These are the initial results from the JET ILW and further work is parts of an ongoing analysis programme of the JET-EFDA Fusion Technology Task Force which continues into the beginning of 2015.

ACKNOWLEDGEMENTS

This work, part-funded by the European Communities under the contract of Association between EURATOM/CCFE was carried out within the framework of the European Fusion Development Agreement. For further information on the contents of this paper please contact publications-officer@jet.efda.org. The views and opinions expressed herein do not necessarily reflect those of the European Commission. This work was also part-funded by the RCUK Energy Programme [grant number EP/I501045].

REFERENCES

[1]. Matthews G.F. et al 2013 Journal of Nuclear Materials **438** S2
[2]. Matthews G.F. et al 2011 Physica Scripta **2011** 014001
[3]. Philipps V. et al these proceedings
[4]. Douai et al 2013 Journal of Nuclear Materials. **438** S1172
[5]. Brezinsek S. et al 2013 Journal of Nuclear Materials **438** S303
[6]. Coad J.P. et al these proceedings
[7]. Ivanova D. et al these proceedings
[8]. Heinola K. et al these proceedings
[9]. Widdowson A. et al 2013 Journal of Nuclear Materials **438** S827 http://dx.doi.org/10.1016/j.jnucmat.2013.01.179
[10]. Arnoux G. et al these proceedings
[11]. Brezinsek S. et al 2013 Nuclear Fusion
[12]. Borodin D. et al these proceedings

[13]. Sergienko G. et al these proceedings
[14]. McCracken G.M. and D.H.J. Goodall 1978 Nucl. Fusion Letters 18 4
[15]. Coad J.P. et al 2011 Physica Scripta **T145** 014003
[16]. Ruset C. et al these proceedings
[17]. Sertoli M. et al these proceedings
[18]. Oberkofler M. et al 2013 Journal of Nuclear Materials **438** S258
[19]. Mayer M. et al 2013 Journal of Nuclear Materials **438** S780 http://dx.doi.org/10.1016/j.jnucmat.2013.01.167

Operating period	Total plasma time (hours)	Divertor phase (hours)	Limiter phase (hours)
2005-2007	35	27	8
2008-2009	45	33	12
2010-2012	19	13	6

Table 1: The total time in divertor and limiter phases for different operating periods.

Operating period	Tile 1*	Tile3 + Tile 1†	Inner ribs	Tile 4	Tile 6	Outer	Tile 7	Tile 8
2008-2009	**55.4**	**73.6**	**75.4**	**329.4**	**316.3**	**45.6**	*-21.3*	*-15.9*
2001-2012	*≥17.8*	<4, *14.6*	2	2, *<4*	2	2	Not measured	Not measured

*Table 2: Comparison of volume of deposition and erosion on divertor tiles from JET-ILW (2011-2012) and JET-C (2008-2009) campaigns. Evaluation of the volume of material eroded or deposited is determined tile by various methods; (i) ion beam analysis (bold), (ii) surface profiling (Italics) and (iii) cross section microscopy (underlined). * Includes major deposition area of tile 1, i.e., the apron and the top thirds of the vertical surface. † Includes tile 3 and the remaining bottom two thirds of the vertical surface of tile 1. Note that values take account of shadowing between tiles where deposits are less than for the remaining surface. The densities used are: for JET-C the density of C deposit* ρ_{Cdep} *= 1g/cm^3; for erosion the density of CFC* ρ_{CFC} *= 1.65g/cm^3 and for JET-ILW the density of Be* ρ_{Be} *= 1.85g/cm^3.*

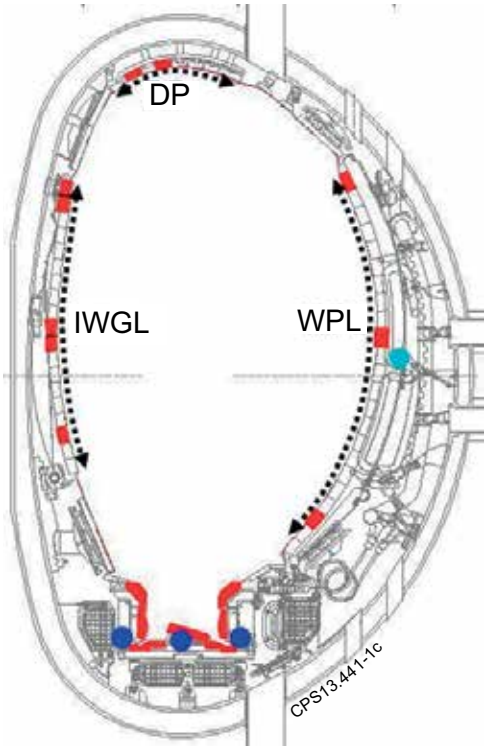

Figure 1. Poloidal cross section of the JET vessel with tile types indicated; (i) Inner Wall Guard Limiter (IWGL), (ii) Dump Plate (DP) & (iii) Wide Poloidal Limiter (WPL). The relative poloidal locations of tiles removed from the vessel for surface analysis are shown in red. Dark blue circles indicate the location of passive diagnostics including test mirrors, sticking deposition monitors, rotating collections and louvre clips. Light blue circle indicates the location of test mirrors and rotating collectors at the outer wall.

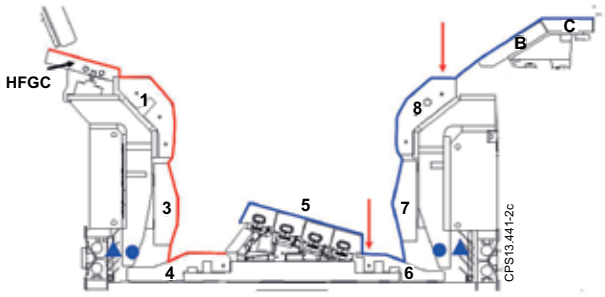

Figure 2. Cross section of the divertor (i) showing the tile numbering and labelling, (ii) location of diagnostics in the remote area at the divertor ribs (blue circle), (iii) location of the remote cooled louver area where louver clips are located (blue triangle), (iv) the toroidal location of delaminations observed on Wcoatings on the apron of tile 8 and the inner edge of tile 6 (red arrow), (v) the surface areas of dust vacuuming shown at the inner divertor in red and the outer divertor in blue. The masses of dust collected from the inner and outer divertor are 0.7g and 0.3g respectively.

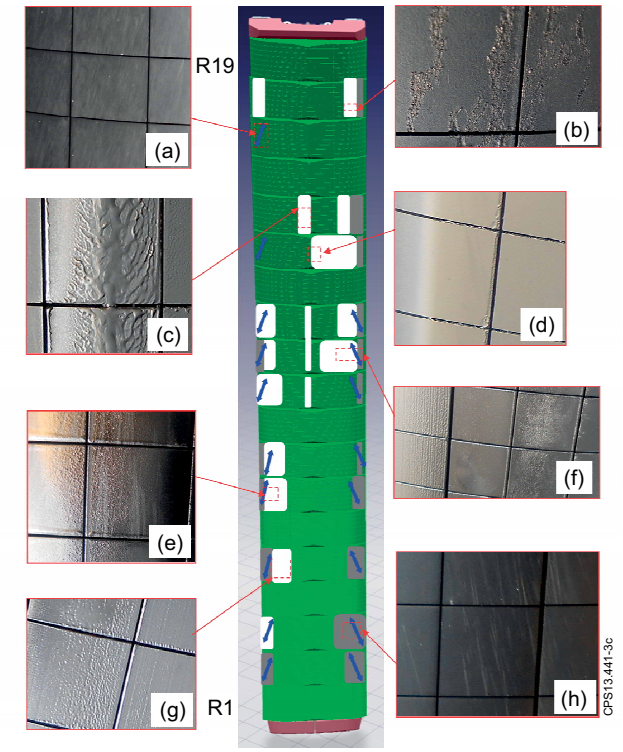

Figure 3. Schematic of IWGL showing surface morphology features on tiles: (a) linear arc tracks on left hand side of IWGL tile; (b) convoluted fern-like arc tracks; (c) melting along toroidal apex with melt bridging gap between catellations; (d) melting along castellation edges; (e) roughening of tile surface; (f) accentuation of machining features (left side of photograph) and roughening of tile surface (right side of photograph); (g) accentuation of machining features; (h) linear arcing on right hand side of IWGL tile. Blue arrows show the orientation of linear arc tracks. White shading shows the location of surface modification through roughening and/or melting. Grey shading indicates visual signs of deposition on tile surface.

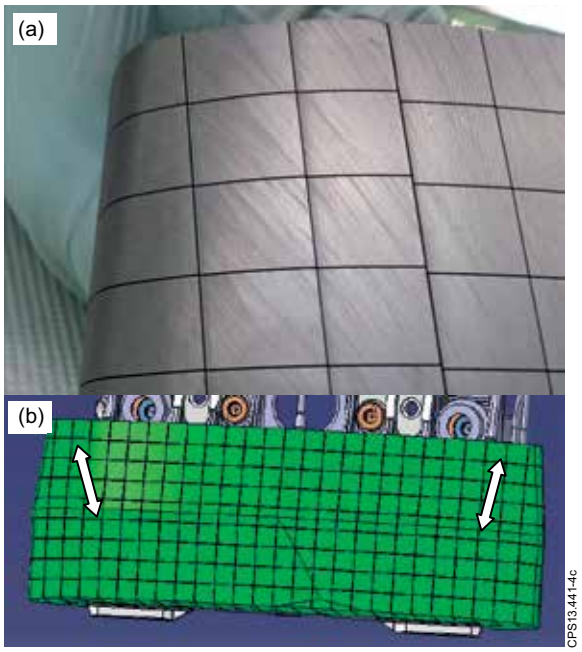

Figure 4. Linear arc tracks on WPL tile.

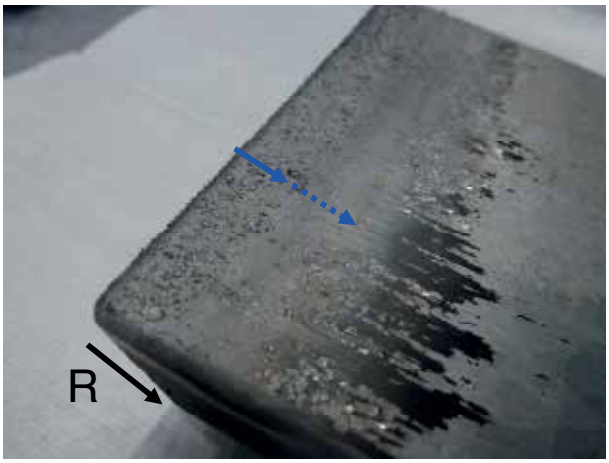

Figure 5. Photograph showing the failure of the W-coating on the shine through protection tile located on the side of a WPL. Solid blue arrow indicates band of Be deposit along the edge of the tile near to the WPL tile. Dashed blue arrow indicates decreasing Be concentration with increasing major radius (R).

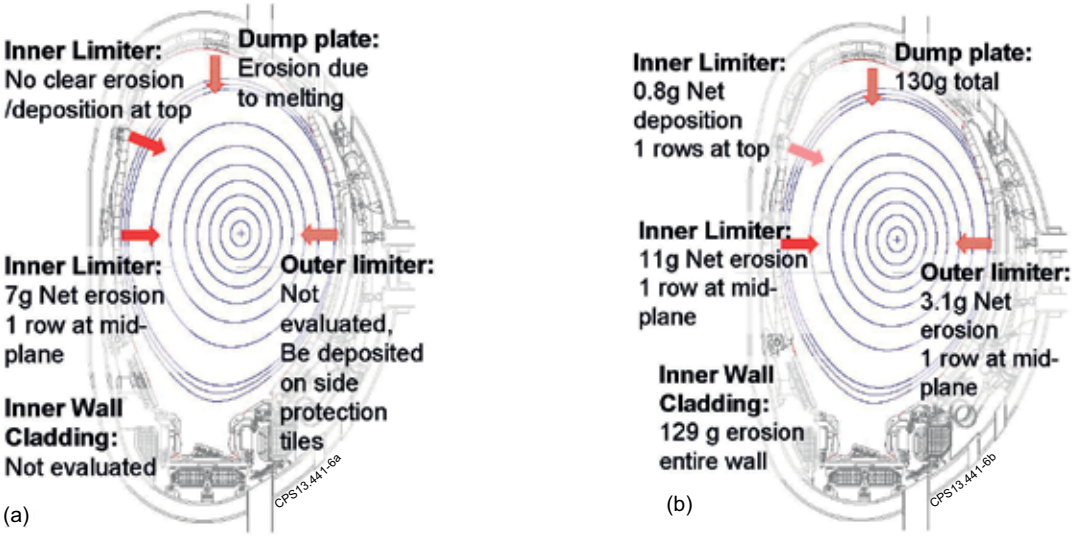

Figure 6. (a) Summary of erosion data for the main chamber of JET from the initial characterisation results from tiles removed from the vessel in 2012. (b) Summary of erosion and deposition data for the main chamber wall for JET-C from the 2008-2009 campaign. Details of the net erosion are taken from [9] and for the inner wall cladding from [19].